Clim Dyn (2011) 36:1475–1489
DOI 10.1007/s00382-010-0816-0

# Changes in Arctic clouds during intervals of rapid sea ice loss

**Steve Vavrus · Marika M. Holland · David A. Bailey**

Received: 1 September 2009 / Accepted: 3 April 2010 / Published online: 22 April 2010


**Abstract** We investigate the behavior of clouds during rapid sea ice loss events (RILEs) in the Arctic, as simulated by multiple ensemble projections of the 21st century in the Community Climate System Model (CCSM3). Trends in cloud properties and sea ice coverage during RILEs are compared with their secular trends between 2000 and 2049 during summer, autumn, and winter. The results suggest that clouds promote abrupt Arctic climate change during RILEs through increased (decreased) cloudiness in autumn (summer) relative to the changes over the first half of the 21st century. The trends in cloud characteristics (cloud amount, water content, and radiative forcing) during RILEs are most strongly and consistently an amplifying effect during autumn, the season in which RILEs account for the majority of the secular trends. The total cloud trends in every season are primarily due to low clouds, which show a more robust response than middle and high clouds across RILEs. Lead-lag correlations of monthly sea ice concentration and cloud cover during autumn reveal that the relationship between less ice and more clouds is enhanced during RILEs, but there is no evidence that either variable is leading the other. Given that Arctic cloud projections in CCSM3 are similar to those from other state-of-the-art GCMs and that observations show increased autumn cloudiness associated with the extreme 2007 and 2008 sea ice minima, this study suggests that the rapidly declining Arctic sea ice will be accentuated by changes in polar clouds.

**Keywords** Arctic · Clouds · Abrupt change · Rapid change · Sea ice · CCSM

S. Vavrus (✉)
Center for Climatic Research, University of Wisconsin, Wisconsin, Madison, USA
e-mail: sjvavrus@wisc.edu

M. M. Holland · D. A. Bailey
National Center for Atmospheric Research, Boulder, USA

## 1 Introduction

Climate change in the Arctic is proceeding at a pace consistent with or even exceeding climate model projections (Serreze et al. 2007, Stroeve et al. 2007, Wang and Overland 2009). Although an amplified polar response to greenhouse forcing has long been simulated by GCMs (Manabe and Stouffer 1980; Mitchell et al. 1990, Holland and Bitz 2003), recent evidence suggests that the transition to a much warmer and less icy state may be punctuated by intervals of rapid climate change. Model simulations of the 21st century have produced these sorts of rapid ice loss events (RILEs) for expected future conditions (Holland et al. 2006; Winton 2006), and some have proposed that the record-setting minimum sea ice coverage during 2007 and 2008 indicates that the system may already be undergoing a "tipping point" of abrupt change (Lindsay and Zhang 2005, Lenton et al. 2008). This recent empirical and theoretical evidence of rapid polar climate shifts is consistent with the paleoclimate record, which shows numerous instances of extremely rapid high-latitude climate variations (e.g., Jansen 1987, Alley et al. 1993, Brook et al. 1996).

The mechanisms for triggering abrupt Arctic climate change have been investigated in many studies and include contributions from the ocean via the meridional overturning circulation (e.g., Manabe and Stouffer 1988), the cryosphere through positive snow- and sea-ice feedbacks

(e.g., Li et al. 2005), the land from methane release in permafrost (Brook et al. 2008), and the atmosphere via shifts in the jet stream (Eisenman et al. 2009). Analyzing RILEs in a set of seven projections of 21st century climate, Holland et al. (2006) identified rapidly increasing poleward ocean heat transport as an important factor in driving episodes of abrupt ice retreat. Likewise, Winton (2006) highlighted surface albedo feedbacks as a key driver in the simulated abrupt elimination of future Arctic sea ice under transient greenhouse forcing.

In contrast, studies of rapid polar climate change have given little consideration to the role that clouds may play, whether as a driver of or responder to RILEs or even as a possible braking mechanism (negative feedback). Given that clouds strongly influence the Arctic radiation budget, have been undergoing discernible trends in recent decades (Schweiger 2004, Wang and Key 2005, Liu et al. 2007), and are expected to change significantly as polar climate evolves in the future (Vavrus et al. 2009a), we feel that an investigation of the relationship between clouds and rapid ice loss is especially timely.

Recent satellite measurements reveal that the extremely low coverage of late-season boreal sea ice during 2007 and 2008 coincided with highly positive cloud anomalies overlying the unusually extensive regions of open water in the Arctic Ocean (Levinson and Lawrimore 2008, Kay and Gettelman 2009). This association agrees with the relationship between changes in sea ice and clouds suggested by the response in transient greenhouse forcing experiments in the Coupled Model Intercomparison Project (CMIP3) archive. Vavrus et al. (2009a) found that the majority of CMIP3 models simulated increasing amounts of clouds in all seasons during the 21st century and that the cloud gains were closely linked to evaporation increases, which appear to provide most of the moisture source for the added cloudiness.

In this paper we explore the behavior of Arctic clouds during intervals of rapid sea ice loss, as simulated by an ensemble of climate model integrations in the Community Climate System Model (CCSM3) for the early-middle 21st century. The major questions we address are the following: (1) What kinds of cloud changes occur during RILEs, compared with the simulated secular trends in clouds?, (2) Do cloud changes amplify or dampen the warming and sea ice loss during RILEs?, (3) How do cloud changes during RILEs vary by season?, and (4) Are clouds acting as a driver of or a responder to the rapid sea ice decreases?

## 2 Model description and experimental design

The CCSM3 is a fully coupled global climate model of the atmosphere, ocean, sea ice, and land systems (Collins et al. 2006a). The atmospheric component is the Community Atmosphere Model, version 3 (CAM3) (Collins et al. 2006b), which employs T85 horizontal resolution ($\sim$1.4°) and 26 levels in a hybrid-sigma pressure coordinate system. The ocean model is POP version 1.4.3 (Smith and Gent 2004), which includes an isopycnal transport parameterization (Gent and McWilliams 1990) and uses a nominal horizontal resolution of 1°. The dynamic-thermodynamic sea ice model—run on the same grid as the ocean component—is the Community Sea Ice Model (CSIM) (Briegleb et al. 2004), whose features include an elastic-viscous-plastic rheology (Hunke and Dukowicz 1997), a sub-gridscale ice thickness distribution (Thorndike et al. 1975) and the thermodynamics of Bitz and Lipscomb (1999). The land component is the Community Land Model (CLM3) (Bonan et al. 2002), which contains ten sub-surface soil layers and computes exchanges of energy, mass, and momentum with the atmosphere. The model uses a sub-grid mosaic of observed plant functional types on the same spatial grid as the atmosphere.

A full description of CAM3's treatment of clouds is given in Collins et al. (2006b) and Boville et al. (2006). Clouds are categorized as either convective or stratiform and are calculated separately at three levels (low, middle, and high). Condensate varies between ice and liquid as a quadratic function of temperature, using threshold temperatures of 243 and 263 K, with different settling velocities for liquid and ice-phase as functions of particle size characterized by the effective radius. The model uses the prognostic cloud-water parameterization of Rasch and Kristjánsson (1998) that was updated by Zhang et al. (2003). CAM3 also includes the radiative effects of aerosols in the calculation of shortwave fluxes and heating rates, based on an aerosol assimilation for the period 1995–2000. The model employs a standard maximum-random cloud overlap scheme (Collins 2001) and separate parameterizations for shallow (Hack 1994) and deep (Zhang and McFarlane 1995) convection. Cloud fraction is determined diagnostically for convective and stratiform clouds, using separate calculations for deep and shallow convection. Stratiform clouds are a function of the grid-box mean relative humidity at each level that varies quadratically from a threshold humidity of 80% over land and 90% elsewhere.

The Arctic cloud simulation of CCSM3 was evaluated by Vavrus and Waliser (2008), who showed that the model produces accurate cloud amounts during summer but overestimates low cloudiness during winter, similar to many GCMs. The monthly total Arctic cloud cover ranges from 70% (December) to 79% (August) averaged over 70–90°N. Walsh et al. (2008) rank CCSM3 as the third best GCM in its simulation of cloud fraction at Barrow, AK, based on a collection of 18 climate models in the CMIP3 collection. CCSM3's liquid cloud condensate and thus

cloud optical depth in the Arctic is known to be too high (Gorodetskaya et al. 2008, Miao and Wang 2008), but its surface cloud radiative forcing compares very favorably to measurements from the AVHRR Polar Pathfinder, outperforming all other GCMs evaluated over ice-covered regions (Karlsson and Svensson 2009).

CCSM3 simulates Arctic sea ice reasonably well compared with late-20th century observations in terms of its spatial distribution and mass budget terms (e.g., Holland et al. 2006, 2008; Gerdes and Koberle 2007). Furthermore, CCSM3 is one of only two CMIP3 models with trends over the latter part of the 20th century that are consistent with the observed satellite era ice loss (Stroeve et al. 2007).

The simulations analyzed here consist of the same seven ensemble members of 21st century simulations used by Holland et al. (2006) to document the characteristics of abrupt reductions in Arctic sea ice in CCSM3. These integrations began from ensembles at the end of 1870–1999 simulations that were driven with observed variations in greenhouse gas concentration, volcanic eruptions, sulfates, ozone, and solar forcing. All seven ensemble members were then forced for the 21st century with the SRES A1B forcing scenario (Nakicenovic et al. 2000), a "middle of the road" case that projects atmospheric $CO_2$ concentrations to rise to 720 ppm by 2100 and aerosol emissions to rise until the 2020s, then decline through 2050 and beyond. Details on the treatment of aerosols in CCSM3 can be found in Collins et al. (2006b).

## 3 Results

### 3.1 Time-mean response to greenhouse forcing

The simulated Arctic cloud response to the projected increases in greenhouse gases by the late 21st century compared with late 20th century conditions is described in detail for the CMIP3 models by Vavrus et al. (2009a). The CCSM3 sea ice response is discussed by Holland et al. (2006). Virtually all boreal sea ice melts off during summer by the end of this century in CCSM3 simulations, although a considerable wintertime ice pack persists (9.9E6 $km^2$ maximum monthly area compared with 13.4E6 $km^2$ in the late 20th century). The typical GCM cloud response during future warming is greater cloudiness in all seasons with a spatial pattern of cloud gains that generally aligns with regions of large sea ice reductions. In the CMIP3 models the greatest cloud increases occur during autumn, correlating with large increases in surface cloud radiative forcing (CRF) that appear to act as a positive feedback on the warming. Increased surface evaporation within the Arctic is the variable most closely associated with the enhanced polar cloudiness. Total cloud increases are mostly attributable to changes at low and high tropospheric levels, but the spatial pattern of the greater vertically integrated cloud amount matches much more closely with the low cloud increase. Winter-time total cloud increases are almost as large as those during autumn, while the smallest and most spatially uniform cloud gain is projected for summer.

CCSM3's time-mean response is similar but accentuated compared with the typical GCM simulation described above. The largest increase in Arctic cloudiness in CCSM3 occurs during autumn and early winter, featuring a sharp rise between September and October that coincides with a very large expansion of open water and enhanced surface evaporation (Fig. 1). The seasonal timing of maximum cloud gains during autumn in CCSM3 not only agrees with the average of CMIP3 models (Vavrus et al. 2009a), but the monthly mean cloud changes through the entire year in CCSM3 correlate with the CMIP3 average values at a robust $r = 0.75$. Over the annual cycle, CCSM3's monthly increases in total cloudiness most closely track the cloud changes at low levels ($r = 0.90$), where the cloud gains are greatest. Clouds at all levels show a noticeable uptick in October, initiating especially large increases in total cloudiness that persist through the winter. The seasonal timing of this accentuated rise in cloud amount has important implications, because the warming influence of Arctic clouds (CRF) peaks during this period (Schweiger and Key 1994; Wang and Key 2005). Thus, the much cloudier conditions simulated during autumn–winter in CCSM3 are suggestive of a positive feedback to the greenhouse warming, similar to the response in the entire CMIP3 model collection (Vavrus et al. 2009a).

### 3.2 Changes during RILEs

The behavior of the Arctic climate system during intervals of abrupt sea ice retreat resembles the time-mean response described above. The similarities are particularly strong during autumn, which is also the most responsive season during RILEs. Because all ten of the RILEs that occur among the seven experiments take place within the first half of the 21st century, the focus of this section will be confined to the years 2000–2049. We also only consider the time-averaged response over three seasons—summer (June–August), autumn (September–November), and winter (December–February)—because the springtime response is much weaker. To more effectively diagnose the impact of cloud changes during summer, we adopt the modified CRF formula of Vavrus (2006), which utilizes downwelling (instead of net) solar radiation to mitigate the competing influence of large surface albedo changes on CRF.

The RILEs analyzed here include all of those identified by Holland et al. (2006), who defined an abrupt event as

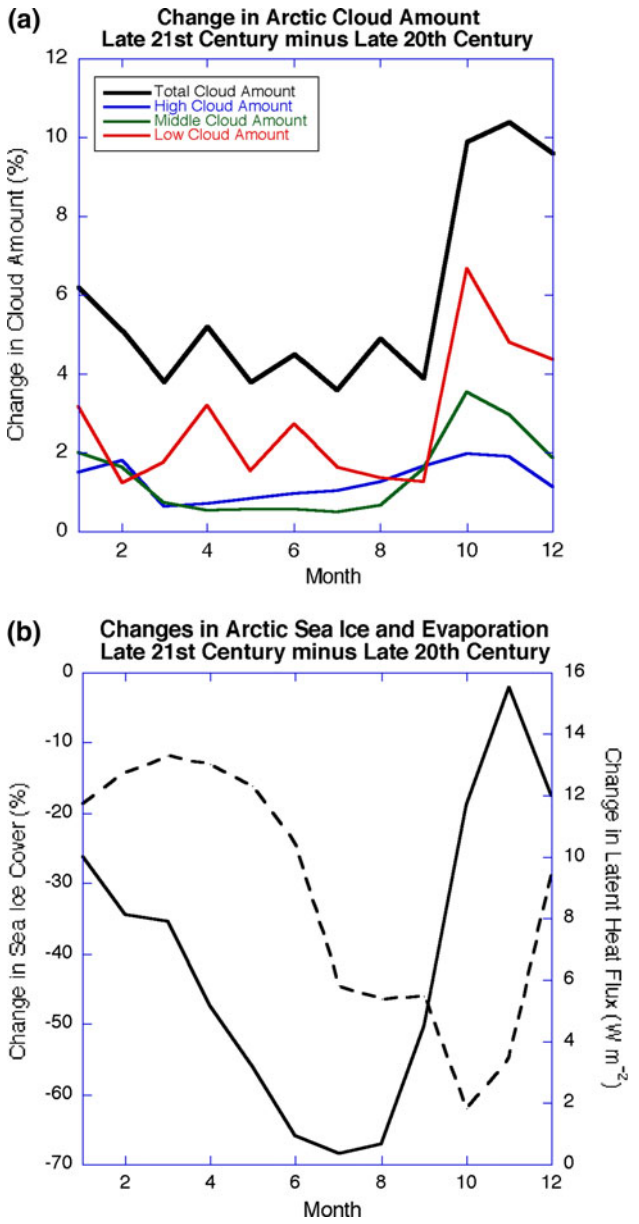


**Fig. 1** The difference in **a** cloud amount and **b** sea ice concentration (*dashed*) and latent heat flux (*solid*) averaged over the Arctic (70–90°N) in CCSM3 between years 2080 and 2099 minus 1980 and 1999 in a transient greenhouse experiment under the SRES A1B emissions scenario

one in which the derivative of the five-year running mean smoothed September ice extent timeseries exceeds a loss of 0.5 million km$^2$year$^{-1}$. In this study we add an additional first event in experiment 2, which nearly meets the above criterion and has been analyzed in detail by Vavrus et al. (2009b). The duration of RILEs ranges from 3 to 9 years (average length 4.8 years), as defined by the time around the transition for which the derivative of the smoothed September ice extent timeseries exceeds a loss of 0.15 million km$^2$ year$^{-1}$ (Holland et al. 2006).

Due to the pronounced secular trends in most variables, we cannot effectively diagnose the behavior of the system by simply comparing averages during RILEs with the multi-decadal averages. Instead, we compare the trends in variables during RILEs versus their 50-year trends to establish the relative response of the system during periods of abrupt change. The ratio of these two trends provides a measure of amplification, such that ratios greater than 1 indicate an enhanced change during RILEs, ratios between 0 and 1 a muted change, and negative ratios a counteracting response.

The sea ice decline during the 2000–2049 time period differs among the ensemble members, although every simulation produces a very substantial decrease in autumn ice concentration (at least 50%) from the beginning of the century and generates at least one interval of accelerated ice loss (Fig. 2). As the autumn sea ice retreats during the course of the early 21st century, the coincident Arctic cloud amount increases in each simulation in a non-monotonic manner that generally accelerates during RILEs. The amplified cloud increase is especially apparent in the second event of experiment 2, both RILEs in experiment 6, and the single event in experiment 7. Overall, the trend in Arctic cloudiness during autumn is much higher during RILEs (0.75% year$^{-1}$) than during the entire first half of the century (0.11% year$^{-1}$), resulting in an amplified gain of 6.66 (Table 1). By comparison, the corresponding amplification factor for the trend of sea ice concentration is smaller (4.66), even though RILEs are defined as intervals of rapid ice loss.

A more detailed understanding of sea ice and cloud behavior during abrupt changes can be derived from the spatial patterns of the secular trends (2000–2049) compared with the trends during RILEs (Fig. 3). During autumn, large decreases of sea ice span almost the entire Arctic Ocean, especially along the ice pack periphery poleward of Siberia and North America (Fig. 3a). This signal is stronger but very similar spatially during RILEs (pattern correlation = 0.92), with maximum declines of up to 10% year$^{-1}$ in the Beaufort and Chukchi Seas that extend to the North Pole. The aforementioned areally averaged total cloud increases are highly variable across the Arctic (Fig. 3b), comprised of maximum gains over the Arctic Ocean that are largely co-located with declining ice concentration. This agreement highlights the important link between cloud generation and enhanced surface evaporation resulting from a diminishing ice pack (Fig. 1; Vavrus et al. 2009a, Sorteberg et al. 2007). The enhanced cloudiness leads to substantially stronger CRF, whose spatial distribution trend during both the early 21st century and RILEs resembles that of total cloud amount, particularly over the ice pack (Fig. 3c). The region with the largest increases of clouds in the central Arctic experiences a

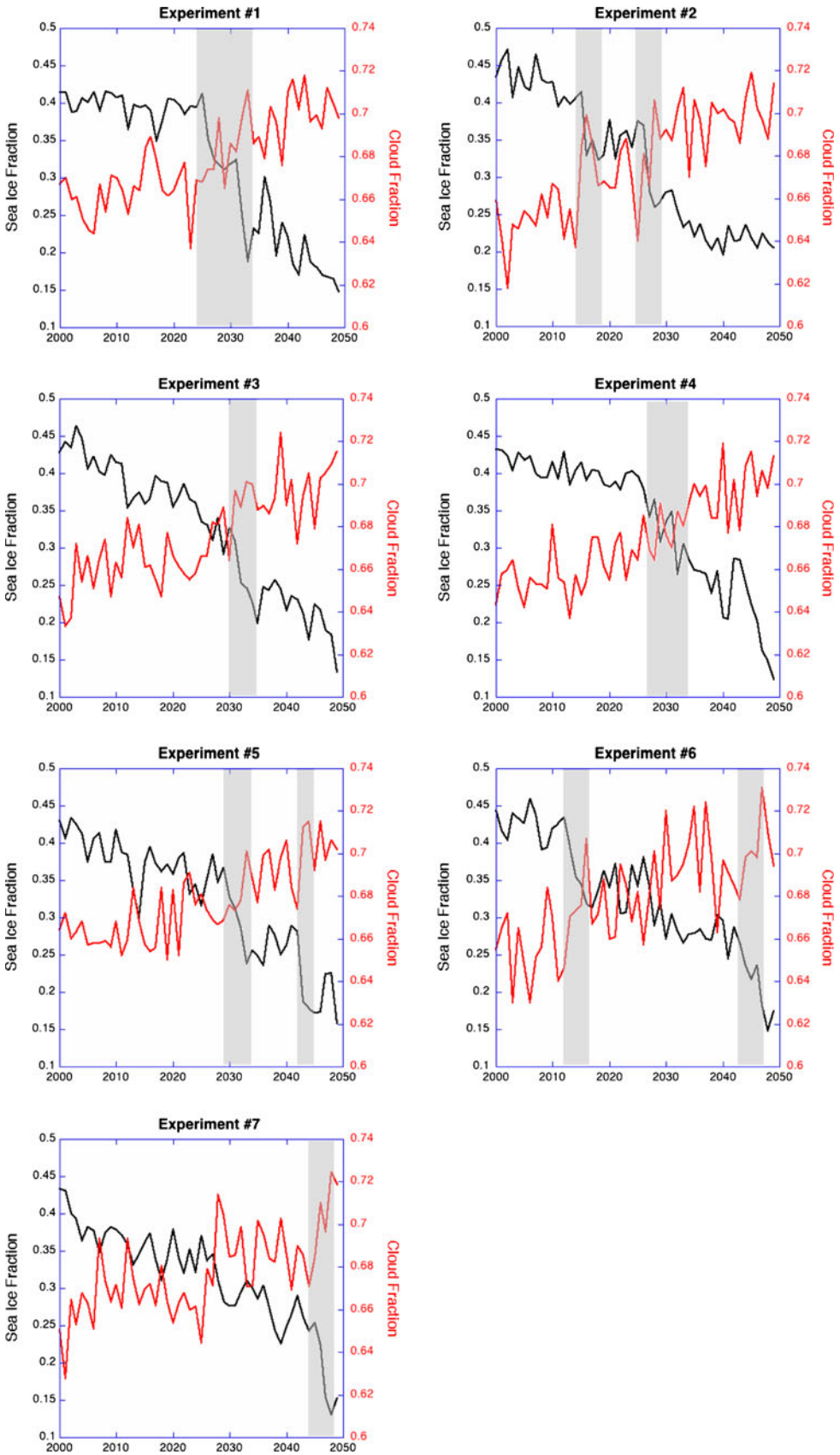


**Fig. 2** Arctic sea ice fraction (*black*) and cloud fraction (*red*) during autumn in seven ensemble members of a 21st-century CCSM3 simulation under greenhouse forcing (SRES A1B scenario). The 10 RILEs are highlighted in *gray*, the fractional values represent averages over 70–90°N, and the time period spans years 2000–2049

**Table 1** Arctic-averaged trends per year (70–90°N) during the first half of the 21st century and during RILEs

| | Mean trend (2000–2049) | Mean trend during RILEs | Ratio of trends | Interquartile range of ratios | Spatial pattern correlation (60–90°N) |
|---|---|---|---|---|---|
| Summer ice cover | −0.35 | −1.53 | 4.33 | 1.90 | 0.83 |
| Summer total cloud | 0.050 | 0.007 | 0.15 | 5.66 | 0.39 |
| Summer low cloud | 0.048 | −0.051 | −1.07 | 6.13 | 0.42 |
| Summer mid cloud | 0.023 | 0.169 | 7.45 | 30.05 | 0.19 |
| Summer high cloud | 0.018 | 0.177 | 10.05 | 24.33 | 0.09 |
| Summer CRF | −0.235 | −0.370 | 1.57 | 4.16 | 0.45 |
| Summer TGCLDIWP | 0.004 | 0.171 | 48.59 | 45.68 | 0.21 |
| Summer TGCLDLWP | 0.274 | 0.227 | 0.83 | 15.83 | 0.20 |
| Autumn ice cover | −0.52 | −2.44 | 4.66 | 2.38 | 0.92 |
| Autumn total cloud | 0.112 | 0.747 | 6.66 | 4.82 | 0.65 |
| Autumn low cloud | 0.115 | 0.778 | 6.79 | 4.89 | 0.68 |
| Autumn middle cloud | 0.044 | 0.185 | 4.25 | 12.06 | 0.00 |
| Autumn high cloud | 0.047 | 0.245 | 5.25 | 7.02 | −0.01 |
| Autumn CRF | 0.068 | 0.539 | 7.94 | 4.36 | 0.82 |
| Autumn TGCLDIWP | 0.017 | 0.115 | 6.82 | 21.06 | 0.21 |
| Autumn TGCLDLWP | 0.817 | 4.424 | 5.41 | 4.74 | 0.58 |
| Winter ice cover | −0.12 | −0.51 | 4.19 | 2.81 | 0.77 |
| Winter total cloud | 0.043 | −0.298 | −6.99 | 22.16 | 0.16 |
| Winter low cloud | 0.030 | −0.133 | −4.39 | 32.91 | 0.19 |
| Winter middle cloud | 0.014 | −0.258 | −18.63 | 43.68 | 0.01 |
| Winter high cloud | 0.036 | −0.421 | −11.82 | 37.73 | 0.04 |
| Winter CRF | 0.090 | 0.094 | 1.05 | 5.48 | 0.35 |
| Winter TGCLDIWP | 0.002 | −0.258 | −142.02 | 160.38 | 0.28 |
| Winter TGCLDLWP | 0.455 | 0.509 | 1.12 | 6.16 | 0.05 |

Values are the mean of all seven ensemble members and all ten RILEs. Also shown are the ratios of the trend during RILEs to the secular trend and the interquartile range of that ratio among the RILEs

The spatial correlation coefficient between the mean secular trend and the mean trend during RILEs is given in the last column and is listed as poleward of 60°N for consistency with Figs. 3–5

*TGCLDIWP* and *TGCLDLWP* are the cloud ice- and liquid–water paths in gm $m^{-2}$. Cloud amounts and sea ice cover are in %, and CRF in W $m^{-2}$, respectively

remarkably large trend in CRF of up to 2 W $m^{-2}$ $year^{-1}$ during RILEs, while the overall spatial pattern of CRF trends during RILEs correlates very highly with the secular trend ($r = 0.82$). We also find a very pronounced overlap between regions of increasing cloudiness and increasing cloud liquid water path (Fig. 3d), whose positive trend is attributable to both the greater amount of clouds and warmer temperatures that shift a larger proportion of the cloud condensate to liquid and thus raise cloud emissivity (Sect. 2). The total cloudiness changes in both time intervals are almost entirely explained by the response of low clouds (Fig. 3e), whereas the spatial trends in middle and high clouds within each time period do not resemble the corresponding patterns of total clouds (Fig. 3f, g). There is also no correlation between the secular trends in high and middle clouds and the corresponding trends of these cloud types during RILES (Table 1). By contrast, the decreasing atmospheric sea level pressure (SLP) over the Arctic Ocean during RILEs (Fig. 3h) is an enhancement of the multi-decadal trend in this region and mostly follows the area of large sea ice reductions (Fig. 3a), consistent with the pressure response associated with sea ice loss identified in other modeling studies (Chapman and Walsh 2007, Deser et al. 2009).

The summertime response bears some resemblance to the autumn patterns, but there are several important differences (Fig. 4). The spatial variations in sea ice decline are similar to those during autumn but the magnitudes are less extreme (Fig. 4a; Table 1). Total cloud amount increases in most regions over the early 21st century, particularly over the Arctic Ocean. During RILEs there are also cloud gains over the ice pack, but generally less cloudy conditions over polar land, especially Siberia and northern Canada (Fig. 4b). Averaged over the Arctic

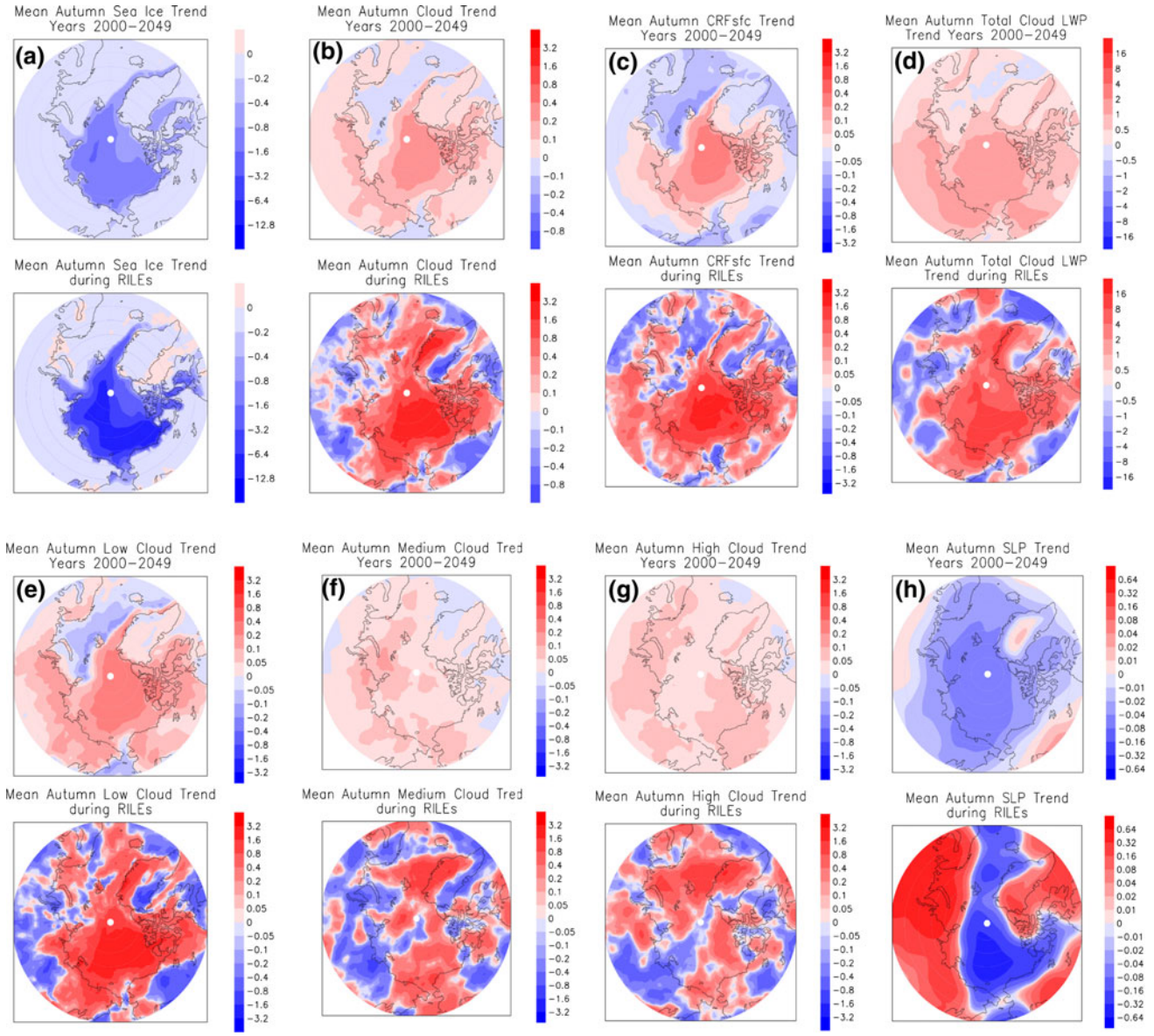


**Fig. 3** Trends in Arctic sea ice, clouds, and circulation during autumn averaged across all seven CCSM3 ensemble members and all ten RILEs. The *upper panel* in each pair represents the trend per year from 2000 to 2049 and the *lower panel* the corresponding trend during RILEs. Shown are **a** sea ice concentration (%); **b** total cloud amount (%); **c** cloud radiative forcing (W $m^{-2}$); **d** total cloud liquid water path (gm $m^{-2}$); **e**–**g** low, middle and high cloud amount (%); and **h** sea level pressure (hPa). Note the geometric scaling in all the plots

(70–90°N), the increasing summertime total cloud amount during RILEs is much smaller than the secular trend (0.007 vs. 0.050% $year^{-1}$) (Table 1). This is explained almost entirely by changes in low clouds (Fig. 4e), which decrease Arctic-wide during RILEs (−0.051% $year^{-1}$) at about the same rate as the multi-decadal increase (0.048% $year^{-1}$). However, this net low-cloud decrease occurs primarily over land and thus affects the ice pack indirectly. The corresponding spatial trends in CRF follow fairly predictably from those of total cloudiness (Fig. 4c), although caution must be exercised in interpreting CRF changes where large decreases in surface albedo occur over the ice pack. As discussed by Rossow and Zhang (1995), changes in surface properties can affect the CRF even in the absence of cloud changes. Consequently, in regions that transition from bright sea ice to dark open ocean, the CRF tends to become considerably more negative, thereby complicating efforts to distinguish the impact of the cloud changes alone. To ameliorate this problem, we apply the modified CRF equation proposed by Vavrus (2006), in which the net solar flux term is replaced with the downwelling solar flux term. Although this approach greatly

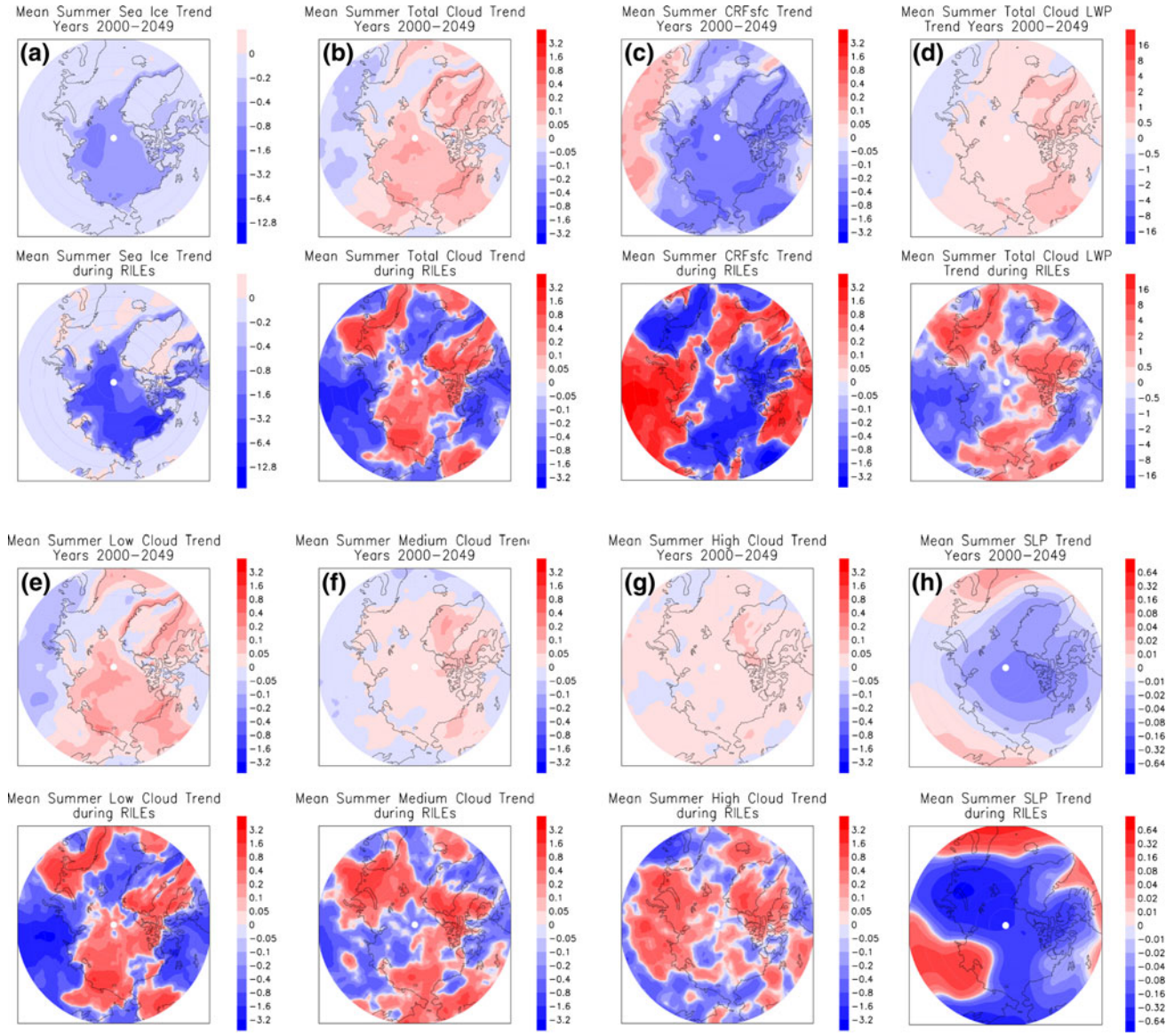


**Fig. 4** As in Fig. 3 but for summer

helps to isolate the effect of cloud changes, some of the decreasing CRF trend over the Arctic Ocean is still likely to be amplified by the reduction in surface albedo. Over land, however, where the CRF changes are easier to interpret, widespread increases in cloud forcing during RILEs of 1–4 W $m^{-2}$ $year^{-1}$ coincide with the declining cloud trend, although this decrease in cloudiness is less robust across RILEs than the increasing cloud trend over the ice pack (not shown). In terms of circulation influences, the declining early 21st-century trend in summertime pressure over the central Arctic and increasing pressure along the periphery is broadly realized during RILEs (Fig. 4h), although the specific features differ. Over the Arctic Ocean there is a general correspondence between decreasing SLP and increasing total cloudiness.

During winter the trends of sea ice and clouds during RILEs are much different than in the other seasons (Fig. 5), and they are more variable across events. In addition, there is generally a weaker wintertime relationship spatially between the secular trends and the changes during RILEs (Table 1). Rather than an extensive region of pronounced sea ice loss across the entire Arctic Ocean, both the multi-decadal and RILE trends show a few distinct maxima along the periphery of the ice pack (Fig. 5a). Over the first half of the century, these extremes are generally associated with relatively large increases in total cloudiness, but the corresponding relationship is less consistent during RILEs (Fig. 5b). Unlike summer and autumn, the areally averaged total cloud amount in winter decreases during RILEs, in sharp contrast to the increasing secular trend (Table 1).

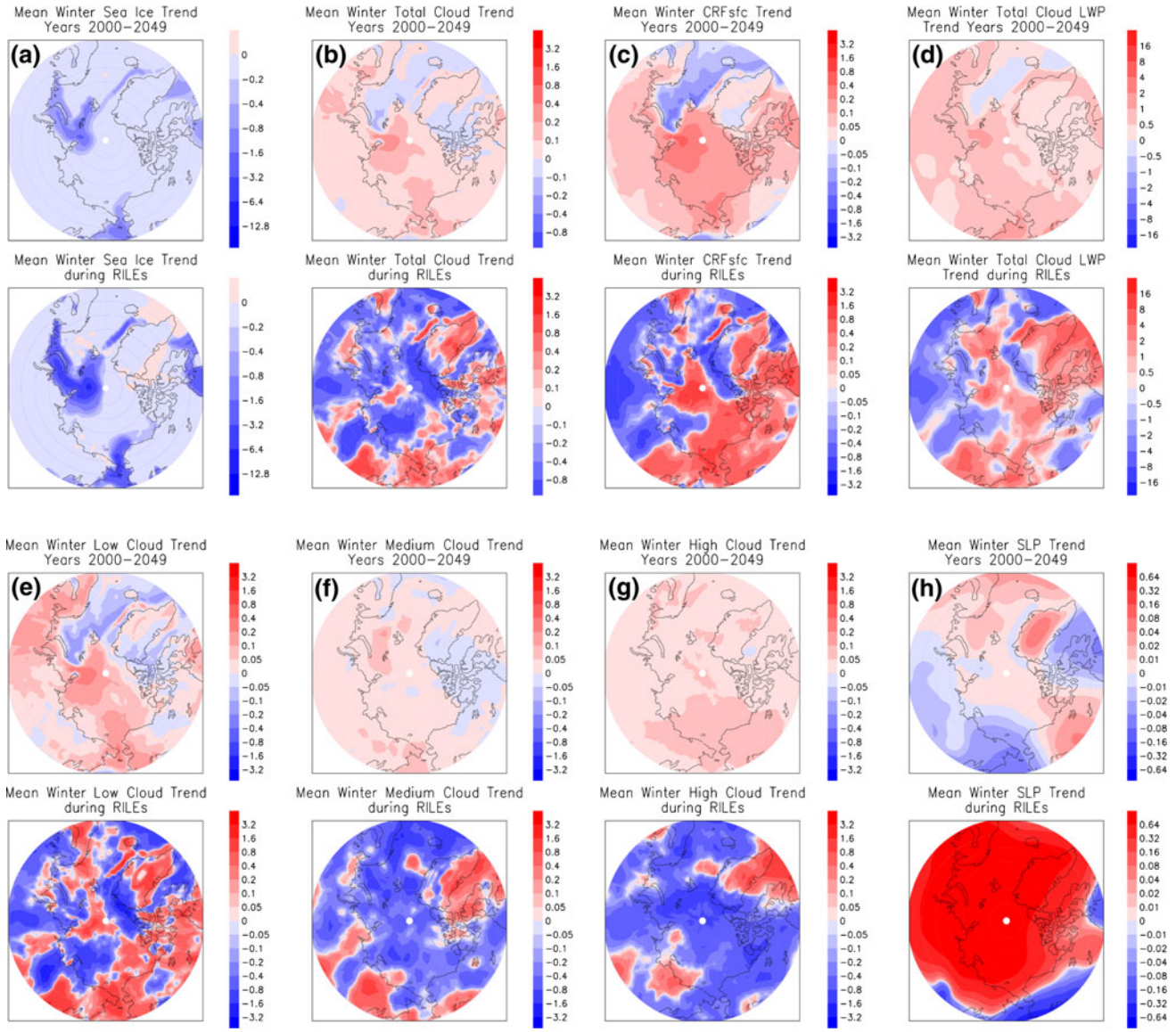


**Fig. 5** As in Fig. 3 but for winter

During RILEs the decreasing total cloudiness Arctic-wide is primarily caused by pronounced reductions in mid-level and upper-level cloudiness, whose negative trends are two to three times larger than that of low clouds (Fig. 5f, g; Table 1). The spatial pattern of total cloud trends during RILEs, however, is similar to the low cloud distribution (Fig. 5e), as is the case in the other seasons.

Part of the reason for the decreasing winter clouds during RILEs may be the pronounced anticyclonic pressure trend, which encompasses almost the entire region poleward of 60°N and maximizes at 1.5 hPa year$^{-1}$ over the Laptev Sea (Fig. 5h). This relationship is consistent with observations showing reduced Arctic winter cloud amount during anticyclonic flow anomalies (Liu et al. 2007). Although somewhat surprising in light of the decreasing pressure trend over the Arctic Ocean during RILEs in summer and autumn, the strongly increasing SLP in winter is consistent with some observational evidence. Francis et al. (2009) showed that atmospheric pressure over the Arctic tends to be significantly higher in the winter following summers with anomalously low sea ice concentration, presumably because enhanced heating of the lower troposphere from expanded open-water coverage increases geopotential heights locally.

Given the decreasing winter cloudiness during RILEs, an unexpected finding is that the CRF trend is positive—and relatively robust among experiments—over most of the polar regions, including the Arctic Ocean (Fig. 5c), at a rate slightly higher than the secular trend (Table 1). A key factor is probably the trend in cloud liquid water path,

which agrees fairly well with the changing CRF and whose (similarly robust) Arctic-averaged amplification factor during RILEs (1.12) is nearly the same as that of CRF (1.05). Apparently, the increasing moisture availability due to expanding open water during RILEs counteracts the radiative effects from the decline in cloud amount, causing the remaining clouds to be more effective heat-trapping agents during winter.

### 3.3 Role of clouds: driver or responder?

The previous sub-section described the simultaneous seasonal behavior of sea ice and clouds during RILEs, but a natural question to ask is whether clouds are simply responding to the rapid ice loss or whether they play a role in driving the ice reductions. To address this question, we calculated lead-lag correlations during autumn, the season when the cloud and sea ice trends are largest and their associations strongest. For each of the seven ensemble simulations and each of the ten RILEs, we correlated the detrended time series of mean monthly Arctic-averaged concentrations of sea ice and total cloudiness during September, October, and November (Tables 2, 3). The relationship between sea ice concentration and cloud amount is fairly weak over the entire 2000–2049 period, consisting of correlation coefficients with magnitudes generally under 0.3, but the data consistently show the expected inverse relationship between sea ice and cloudiness. Across all time lags, the correlations are strongest for November cloud amount (−0.35) and weakest for September clouds (−0.18). Comparing the average of the three correlations showing no time lag, the three with sea ice leading clouds, and the three with clouds leading sea ice (Fig. 6), we find very similar values ($r = -0.27$, $-0.27$, and $-0.20$, respectively) that provide no clear evidence of one variable acting as a driver.

The corresponding correlations averaged over the ten RILEs demonstrate that a much stronger relationship emerges when the ice coverage is rapidly declining (Table 3). The magnitude of all the coefficients is at least 0.3 and exceeds 0.5 in several cases. Correlations averaged across all time lags are again largest for November cloud amount (−0.57), and they are higher in every month during RILEs than the corresponding values across the entire pre-2050 time frame. Again comparing the average of the correlations showing no time lag, sea ice leading clouds, and clouds leading sea ice (Fig. 6), we find that these relationships are almost twice as strong ($r = -0.48$) during RILEs than during the whole 50-year record, but curiously these three different lead-lag correlations during RILEs are identical. This match indicates that at least on the monthly timescales considered here, there is no evidence to resolve the question of whether the pronounced autumn sea ice and cloudiness anomalies during RILEs are triggered by the ice or the clouds. This result suggests that the very rapid response of surface radiative fluxes to changes in cloudiness in the Arctic (Intrieri et al. 2002) necessitates that lead-lag correlations be calculated at higher temporal resolution, but unfortunately daily output from these simulations was not available. We also acknowledge that other sea ice variables such as freeze-up date and growth rates might be more sensitive to the warming influence of

**Table 2** Ensemble-mean, detrended lead-lag correlations between the average monthly Arctic sea ice concentration and total cloud amount (70–90°N) during autumn between 2000 and 2049

| Cloud amount | | | |
|---|---|---|---|
| Ice concentration | September | October | November |
| September | −0.13 | −0.19 | −0.26 |
| October | −0.25 | −0.27 | −0.36 |
| November | −0.16 | −0.20 | −0.42 |
| *Seasonal mean* | *−0.18* | *−0.22* | *−0.35* |

**Table 3** Ensemble-mean, detrended lead-lag correlations between the average monthly Arctic sea ice concentration and total cloud amount (70–90°N) during autumn among all RILEs

| Cloud amount | | | |
|---|---|---|---|
| Ice concentration | September | October | November |
| September | −0.45 | −0.30 | −0.51 |
| October | −0.59 | −0.45 | −0.64 |
| November | −0.46 | −0.39 | −0.55 |
| *Seasonal Mean* | *−0.50* | *−0.38* | *−0.57* |

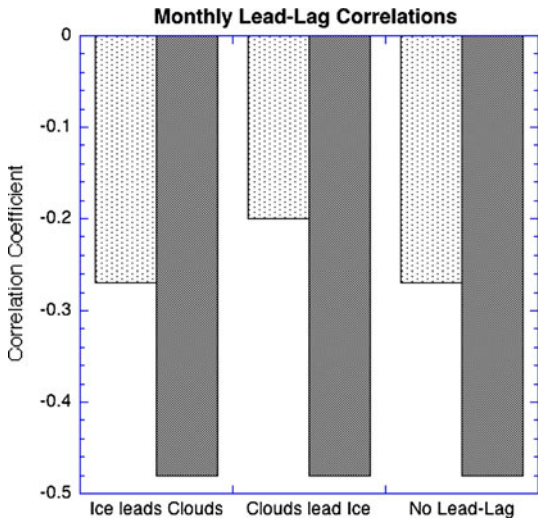


**Fig. 6** Summary of monthly lead-lag correlations between Arctic sea ice concentration and total cloud amount during autumn over the entire 2000–2049 period (*stippled*) and during RILEs (*solid*)

increased autumn cloudiness, but we retain ice concentration as our comparative metric due to its close physical linkage with surface evaporation and therefore cloud formation.

A further way of measuring the sea ice-cloud coupling and the possible role of clouds in that relationship is to consider the reverse correlation: how does sea ice vary during intervals of extremely rapid cloud increases (during autumn)? To address this question, we identified the 10 intervals of most rapid autumn cloud increases, based on the average cloud fraction trends over a 3- to 9- year window to match the range of the 10 RILEs. We find that the average interannual trend in autumn ice fraction among these 10 "rapid cloud gain events" ($-0.015$ year$^{-1}$) is nearly three times larger than the corresponding ice-fraction trend over the entire 50-year simulation ($-0.0052$ year$^{-1}$). Furthermore, the rate of ice loss during autumn in all 10 of these cases exceeds the 50-year average ice-fraction trend, and the majority of these cases (6 out of 10) coincide with the 10 RILEs. Moreover, the magnitude of the ice-loss trends during seven of these ten events is among the maximum 10% of all the trends simulated across the ensemble members. These results demonstrate that the strong relationship we identified between extremely rapid sea ice reductions and large cloud increases also operates in reverse—i.e., extremely rapid (autumn) cloud increases coincide with large reductions in sea ice. This finding underscores the close sea ice-cloud association and suggests that increasing autumn cloudiness may be more than a passive response to abrupt declines in Arctic sea ice.

## 4 Synthesis and discussion

The model simulations strongly suggest that certain predictable features of the Arctic climate system are likely to develop during intervals of abrupt sea ice reductions. The strongest and most robust signal of cloud changes occurs in autumn, when the secular trend of increasing clouds at all levels is enhanced during RILEs, along with an amplification of cloud radiative forcing and cloud water- and ice content. In a comparison of all the seasons, autumn stands out not only in terms of the pronounced amplification of the trends during RILEs but also with respect to the consistency of the amplification factors among all variables and the robustness across the ensemble members (Fig. 7; Table 1). Unlike summer and winter, during autumn all of the amplification factors are much larger than one, and almost all exceed the benchmark ratio for sea ice concentration (4.66). They also display a remarkably small range: minimum ratio of 4.25 for middle cloud amount and a maximum ratio of 7.94 for CRF. In contrast, the amplification factors vary widely during summer—between $-1.07$

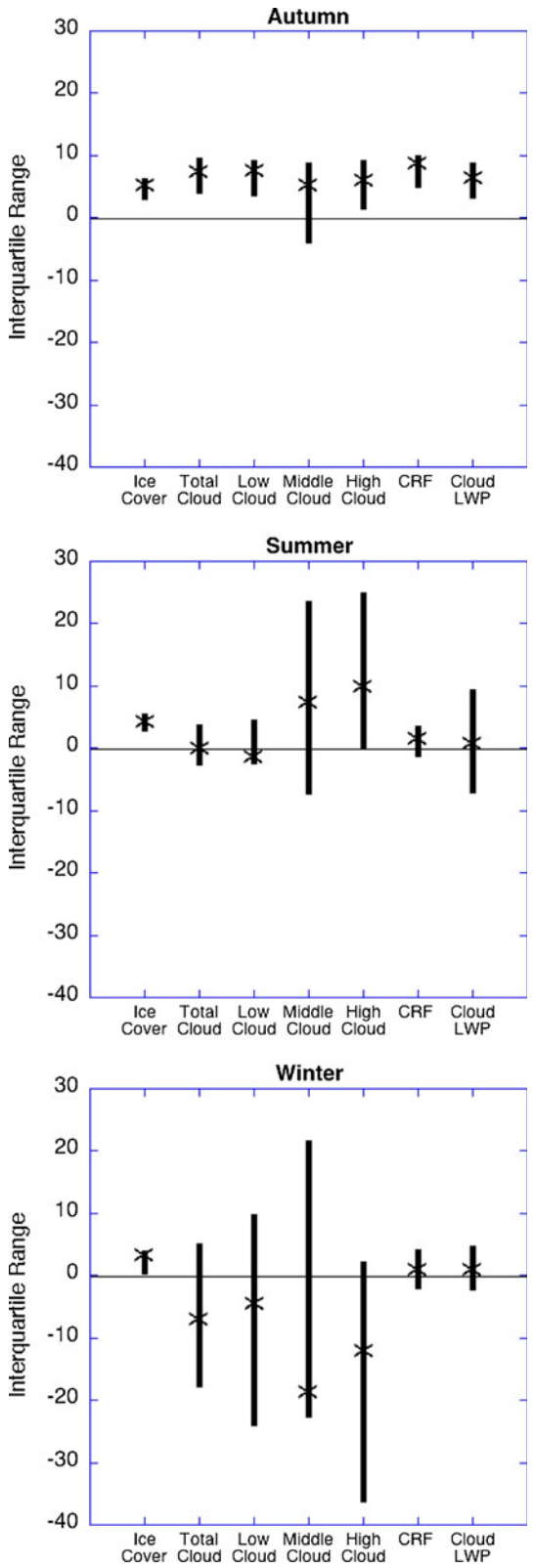


**Fig. 7** Ratio of trends during RILEs versus secular trends during (*top*) autumn, (*middle*) summer, and (*bottom*) winter, as expressed by the ensemble mean ("*X*") and interquartile range. Due to the skewed distribution of the ratios, the mean value is often not centered about the interquartile range

(low cloud amount) and 48.59 (cloud ice-water path), and even more during winter—between −142.02 (cloud ice-water path) and 1.12 (cloud liquid–water path). The much more consistent autumnal response among the cloud properties also holds across the ensemble members, indicating a particularly robust signal during this season (Fig. 7). The interquartile ranges of the amplification factors across all seven ensemble members are considerably smaller during autumn than in either other season for almost every variable, while the summertime changes are more robust than those in winter (Fig. 7; Table 1). The trends in middle and high clouds show relatively large scatter across RILEs during every season, whereas CRF consistently exhibits the smallest variability among cloud properties—even during winter, when the trends in cloud amounts vary widely among the simulations.

Autumn also stands out in terms of the strong influence of RILEs on the 50-year trends. For every sea ice and cloud variable, the majority of the changes from 2000 to 2049 are accounted for by the trends during RILEs (Fig. 8). The contributions from abrupt events exceed 60% for each term and are especially large for total and low clouds (>80%), resulting in the secular trend in CRF being entirely explained by the large increases that occur during RILEs.

An important question is whether the cloud changes during RILEs act as a feedback mechanism to enhance or mitigate the transient shift of the Arctic toward a warmer, less icy state. Although we forego a formal feedback analysis in this study, our results suggest that clouds generally reinforce the declining trends of sea ice during RILEs. This conclusion is strongest for autumn, when the cloud changes are largest and most consistent and the CRF is comprised almost entirely of the (warming) longwave radiation term. CCSM3 simulates its largest positive CRF during autumn with a maximum of over 40 W $m^{-2}$ in October, in agreement with satellite observations (Karlsson and Svensson 2009). The amplified cloud increases in autumn during RILEs should therefore boost the rapid ice reductions by more effectively trapping the outgoing surface longwave energy and re-radiating some of it back to the surface. The particularly pronounced increases in autumn CRF during RILEs (eight times as large as the secular trend) underscores this mechanism.

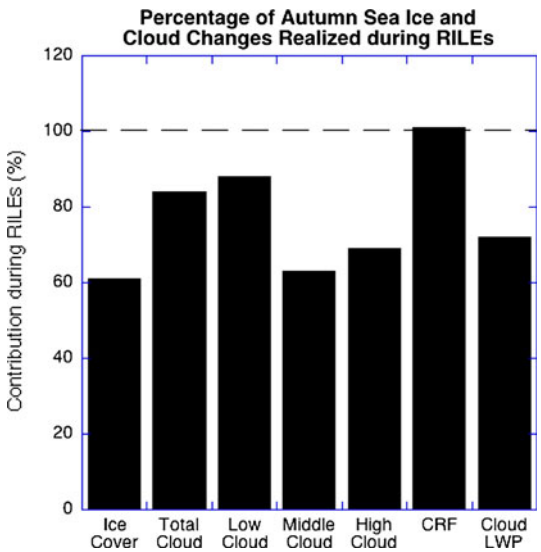


**Fig. 8** Contribution from RILEs to the autumn sea ice and cloud changes during 2000 to 2049. The years in which there were RILEs accounted for 14% of the 50-year period averaged among the seven ensemble members

In other seasons the evidence for a cloud feedback is less obvious, but during summer the rate of increase in total cloudiness during RILEs is only 15% as large as the secular trend in this season when clouds cool the surface (Schweiger and Key 1994), and the increasing rate of cloud liquid water during RILEs is also smaller than the multi-decadal rate. Furthermore, although summertime low clouds increase over the first half of the 21st century, they decrease on average Arctic-wide during RILEs. Because Arctic low-level clouds are the predominant and most radiatively significant cloud type (Uttal et al. 2002), their decline means that more solar energy can reach the surface during summer and thus enhance warming (we note, however, that in our simulations most of this extra heating would have to be transmitted indirectly to the ice surface because the reduced summertime total cloudiness during RILEs occurs primarily over land) (Sect. 3.2). This interpretation of the summer feedback role of clouds in RILEs is complicated by the amplified negative trend in CRF during this season (Table 1), but changes in CRF when sunlight is present are known to be strongly influenced by changes in surface albedo and thus provide no simple explanation for the influence of the cloud response itself (Sect. 3.2). In winter, clouds decrease during RILEs at every level in conjunction with rising atmospheric pressure, seemingly favoring sea ice growth over this season in which clouds strongly warm the Arctic surface. We remind the reader, however, that in winter the areally averaged trend in CRF is slightly more positive during RILEs than over the early 21st century (Sect. 3.2), presumably due to the similar sized amplification of the cloud liquid water trend. These magnified positive trends in CRF and liquid condensate are also relatively robust (Fig. 7) and suggest that cloud changes in this season may still serve as a positive feedback, despite the overall decreasing trend in winter cloud amount.

Although this study is focused on model simulations and thus inherently restricted, we are encouraged by the agreement between some of our major findings and the limited record of cloud-ice interactions when open water in the Arctic is unusually expansive. Following the record-

setting Arctic sea ice minimum in 2007, cloudiness was observed to increase substantially during autumn over areas of ice loss (Levinson and Lawrimore 2008), similar to the simulated response during RILEs. Cloud cover was unusually sparse over the Arctic during summer 2007, possibly playing a similarly important role in generating large amounts of ice melt (Kay et al. 2008). An analogous process may be operative in our simulations, although most of the negative cloud anomalies in summer 2007 occurred over sea ice, whereas the decreasing trend in low clouds during RILEs is primarily land-based. A slightly broader observational study covering 2006–2008 conditions (Kay and Gettelman 2009) shows considerably greater amounts of low clouds over the Arctic Ocean during early autumn in the low-ice years of 2007 and 2008, compared with the much icier conditions in 2006. Similarly, satellite lidar data from 2003 to 2007 show a greater amount of low clouds during mid-autumn over open water than above sea ice (Palm et al. 2009). Given the pronounced downward trend of Arctic ice extent in recent years (Stroeve et al. 2007), we expect that more opportunities will arise in the near future to monitor the relationship between polar clouds and sea ice during times of anomalously low ice coverage.

## 5 Conclusions

Because the Arctic system may already be starting an abrupt transition toward a much warmer and less icy climate than at any time in the recent past, we need to understand the mechanisms that could drive this shift. Our study considers the role of clouds during such environmental changes, utilizing multiple realizations of the 21st century in CCSM3. By comparing trends in cloud properties during RILEs with their more gradual evolution over the course of the early 21st century, we identify major features that may improve understanding of the role of clouds in rapid Arctic climate change.

The results of this study support the following conclusions:

- Clouds should increase in the Arctic as the climate warms, and the trend toward cloudier conditions will probably be most pronounced during autumn due to the maximum enhancement of evaporation during that season.
- During RILEs, clouds are also expected to increase most in autumn, resulting in a potentially important positive feedback that hinders freeze-up and thus favors thinner ice.
- The autumn cloud expression during RILEs is the most robust of any season, in terms of inter-ensemble spread and the consistency among the cloud amplification factors (cloud amount, water content, and radiative forcing).
- During autumn, most of the changes in sea ice and cloud variables over the first half of the 21st century are realized during RILEs, including the entire secular trend in CRF.
- The trends in total cloudiness during RILEs are explained almost entirely by the response of low-level clouds, rather than by middle or high clouds, and the low cloud trends show the most consistency among the simulations.
- No clear lead-lag relationship is evident in autumn between changes in the coverage of sea ice and clouds during RILEs, indicating that at least on monthly timescales the two vary nearly synchronously, although the strength of the sea ice-cloud correlations is much greater when the ice coverage is rapidly declining. On seasonal timescales, however, the results suggest a possible cause-and-effect, in that decreasing low cloudiness in summer during RILEs may promote less sea ice and more clouds during autumn.
- Cloud changes appear to accelerate the rapid loss of sea ice at least during autumn and possibly in winter. Both enhanced autumn cloudiness trapping more outgoing longwave radiation and increasing amounts of liquid cloud condensate during winter lead to an amplified increase in CRF. The corresponding role of clouds during summer is less certain, but the relatively smaller increase in total clouds and the decreasing trend in low clouds during RILEs suggests that a positive feedback could also be at work in that season.
- A positive feedback from primarily low cloud changes amid a warming climate is supported by other GCM simulations of the Arctic's transient and time-mean response to greenhouse forcing (e.g., Miller and Russell 2002, Vavrus 2004), in addition to a recent observational/modeling study of subtropical low-level cloud trends in recent decades (Clement et al. 2009). We know of no other previous studies, however, that have investigated the role of polar clouds during abrupt climate change.
- The similarity of CCSM3's future transient cloud response with those of other GCMs in the CMIP3 archive and the strong resemblance between our major simulated features and observations during the low-ice years of 2007–2008 suggest that clouds should be considered an important candidate among the processes hastening the retreat of Arctic sea ice. Future research could investigate whether a similar relationship exists between clouds and sea ice in the other six CMIP3 climate models exhibiting abrupt ice retreat during their 21st century simulations (Holland et al. 2006).

**Acknowledgments** This study was supported by grants from the National Science Foundation (OPP-0327664, OPP-0612388, ARC-0628910, and ARC-0652838). MM Holland was supported by NASA grant NNG06GB26G. This work was also made possible by the support of UCAR through its Faculty Fellowship Program, which allowed the authors to collaborate on this project while Vavrus was a visiting scientist at NCAR.

## References

Alley RB, Meese DA, Shuman CA, Gow AJ, Taylor KC, Grootes PM, White JWC, Ram M, Waddington ED, Mayewski PA, Zielinski GA (1993) Abrupt increase in Greenland snow accumulation at the end of the Younger Dryas event. Nature 362:527–529

Bitz CM, Lipscomb WH (1999) An energy-conserving thermodynamic model of sea ice. J Geophys Res 104:15669–15677

Bonan GB, Oleson KW, Vertenstein M, Levis S, Zeng X, Dai Y, Dickinson RE, Yang Z-L (2002) The land surface climatology of the Community Land Model coupled to the NCAR Community Climate Model. J Clim 15:3123–3149

Boville BA, Rasch PJ, Hack JJ, McCaa JR (2006) Representation of clouds and precipitation processes in the Community Atmosphere Model (CAM3). J Clim 19:2184–2198

Briegleb BP, Bitz CM, Hunke EC, Lipscomb WH, Holland MM, Schramm JL, Moritz RE (2004) Scientific description of the sea ice component of the Community Climate System Model, version 3. Tech Rep NCAR/TN-463+STR, National Center for Atmospheric Research, Boulder, pp 78

Brook EJ, Sowers T, Orchardo J (1996) Rapid variations in atmospheric methane concentration during the past 110 ka. Science 273:1087–1091

Brook E, Archer D, Dlugokencky E, Frolking S, Lawrence D (2008) Potential for abrupt changes in atmospheric methane. In: Abrupt climate change, a report prepared by the US Climate Change Science Program and the Subcommittee on Global Change Research. US Geological Survey, Reston, pp 360–452

Chapman WL, Walsh JE (2007) Simulations of Arctic temperature and pressure by global coupled models. J Clim 20:609–632

Clement AC, Burgman R, Norris JR (2009) Observational and model evidence for positive low-level cloud feedback. Science 325:460–464

Collins WD (2001) Parameterization of generalized cloud overlap for radiative calculations in general circulation models. J Atmos Sci 58:3224–3242

Collins WD, Bitz CM, Blackmon ML, Bonan GB, Bretherton CS, Carton JA, Chang P, Doney SC, Hack JJ, Henderson TB, Kiehl JT, Large WG, McKenna DS, Santer BD, Smith RD (2006a) The Community Climate System Model: CCSM3. J Clim 19:2122–2143

Collins WD, Rasch PJ, Boville BA, Hack JJ, McCaa JR, Williamson DL, Briegleb BP, Bitz CM, Lin S-J, Zhang M (2006b) The formulation and atmospheric simulation of the Community Atmospheric Model version 3 (CAM3). J Clim 19:2144–2161

Deser C, Tomas R, Alexander M, Lawrence D (2009) The seasonal atmospheric response to projected Arctic sea ice loss in the late 21st century. J Clim 23:333–351

Eisenman I, Bitz CM, Tziperman E (2009) Rain driven by receding ice sheets as a cause of past climate change. Paleoceanography 24. doi:10.1029/2009PA001778

Francis JA, Chan W, Leathers DJ, Miller JR, Veron DE (2009) Winter Northern Hemisphere weather patterns remember summer Arctic sea-ice extent. Geophys Res Lett 36:L07503. doi:10.1029/2009GL037274

Gent PR, McWilliams JC (1990) Isopycnal mixing in ocean circulation models. J Phys Oceanogr 20:150–155

Gerdes R, Koberle C (2007) Comparison of Arctic sea ice thickness variability in IPCC climate of the 20th century experiments and in ocean-sea ice hindcasts. J Geophys Res 112:C04S13. doi:10.1029/2006JC003616

Gorodetskaya IV, Tremblay L-B, Liepert B, Cane MA, Cullather RI (2008) Modification of the Arctic Ocean short-wave radiation budget due to cloud and sea ice properties in coupled models and observations. J Clim 21:866–882

Hack JJ (1994) Parameterization of moist convection in the NCAR Community Climate Model, CCM2. J Geophys Res 99(D3):5551–5568

Holland MM, Bitz CM (2003) Polar amplification of climate change in the coupled model intercomparison project. Clim Dyn 21:221–232

Holland MM, Bitz CM, Tremblay B (2006) Future abrupt reductions in the summer Arctic sea ice. Geophys Res Lett 33:L23503. doi:10.1029/2006GL028024

Holland MM, Serreze MC, Stroeve J (2008) The sea ice mass budget of the Arctic and its future change as simulated by coupled climate models. Clim Dyn. doi:10.1007/s00382-008-0493-4

Hunke EC, Dukowicz JK (1997) An elastic-viscous-plastic model for sea ice dynamics. J Phys Oceanogr 27:1849–1867

Intrieri JM, Fairall CW, Shupe MD, Persson POG, Andreas EL, Guest PS, Moritz RM (2002) An annual cycle of Arctic surface cloud forcing at SHEBA. J Geophys Res 107(C10). doi:10.1029/2000JC000439

Jansen E (1987) Rapid changes in the inflow of Atlantic water into the Norwegian Sea at the end of the last glaciation. In: Berger WH, Labeyrie LD (eds) Abrupt climatic change. Reidel, Dordrecht, pp 299–310

Karlsson J, Svensson G (2009) The simulation of Arctic clouds and their influence on the winter surface temperature in present-day climate in the CMIP3 multi-model dataset. Clim Dyn. doi:10.1007/s00382-010-0758-6

Kay JE, Gettelman A (2009) Cloud influence on and response to seasonal Arctic sea ice loss. J Geophys Res. doi:10.1029/2009JD011773

Kay JE, L'Ecuyer T, Gettelman A, Stephens G, O'Dell C (2008) The contribution of cloud and radiation anomalies to the 2007 Arctic sea ice extent minimum. Geophys Res Lett 35:L08503. doi:10.1029/2008GL033451

Lenton TM, Held H, Kriegler E, Hall JW, Lucht W, Rahmstorf S, Schellnhuber HJ (2008) Tipping elements in the Earth's climate system. Proc Nat Acad Sci 105(6):1786–1793

Levinson DH, Lawrimore JH (2008) State of the climate in 2007. Bull Am Met Soc 89:S1–S179. doi:10.1175/BAMS-89-7-StateoftheClimate

Li C, Battisti D, Schrag D, Tziperman E (2005) Abrupt climate shifts in Greenland due to displacements of the sea ice edge. Geophys Res Lett 32:L19702. doi:10.1029/2005GL023492

Lindsay RW, Zhang J (2005) The thinning of Arctic sea ice, 1988–2003: have we passed a tipping point? J Clim 18:4879–4894

Liu Y, Key JR, Francis JA, Wang X (2007) Possible causes of decreasing cloud cover in the Arctic winter, 1982–2000. Geophys Res Lett 34:L14705. doi:10.1029/2007GL030042

Manabe S, Stouffer RJ (1980) Sensitivity of a global climate model to an increase of $CO_2$ concentration in the atmosphere. J Geophys Res 85:5529–5554

Manabe S, Stouffer RJ (1988) Two stable equilibria of a coupled ocean-atmosphere model. J Clim 1:841–866

Miao Q, Wang Z (2008) Comparison on cloud and radiation properties at Barrow between ARM/NSA measurements and GCM outputs. 18th Atmospheric Radiation Measurement (ARM) Science Team Meeting, Norfolk

Miller JR, Russell GL (2002) Projected impact of climate change on the energy budget of the Arctic Ocean by a global climate model. J Clim 15:3028–3042

Mitchell JFB, Manabe S, Meleshko V, Tokioka T (1990) Equilibrium climate change and its implications for the future. In: Houghton JT, Jenkins GJ, Ephraums JJ (eds) Climate Change: The IPCC Scientific Assessment. Cambridge University Press, Cambridge, pp 131–172

Nakicenovic N et al (2000) Special report on emissions scenarios: a special report of Working Group III of the Intergovernmental Panel on Climate Change. Cambridge University Press, pp 599

Palm SP, Marshak A, Yang Y, Spinhirne J, Markus T (2009) The influence of Arctic sea ice extent on polar cloud fraction and vertical structure and implications for regional climate. Proceedings of the 10th conference on polar meteorology and oceanography, American Meteorological Society, Madison, WI

Rasch PJ, Kristjánsson JE (1998) A comparison of the CCM3 model climate using diagnosed and predicted condensate parameterizations. J Clim 11:1587–1614

Rossow WB, Zhang YC (1995) Calculation of surface and top of atmosphere radiative fluxes from physical quantities based on ISCCP data sets, 2: validation and first results. J Geophys Res 100(D1):1167–1197

Schweiger AJ, Key J (1994) Arctic Ocean radiative fluxes and cloud forcing estimated from the ISCCP C2 cloud data set, 1983–1990. J Appl Meteorol 33:948–963

Schweiger A (2004) Changes in seasonal cloud cover over the Arctic seas from satellite and surface observations. Geophys Res Lett 31:L12207. doi:10.1029/2004GL020067

Serreze MC, Holland MM, Stroeve J (2007) Perspectives on the Arctic's shrinking sea-ice cover. Science 315:1533–1536

Smith R, Gent P (2004) Reference manual for the parallel ocean program (POP) ocean component of the Community Climate System Model (CCSM2.0 and 3.0), LAUR-02–2484. Los Alamos National Laboratory, Los Alamos

Sorteberg A, Kattsov V, Walsh JE, Pavlova T (2007) The Arctic surface energy budget as simulated with the IPCC AR4 AOGCMs. Clim Dyn 29:131–156

Stroeve J, Holland MM, Meier W, Scambos T, Serreze M (2007) Arctic sea ice decline: faster than forecast. Geophys Res Lett 34:L09501. doi:10.1029/2007GL029703

Thorndike AS, Rothrock DA, Maykut GA, Colony R (1975) The thickness distribution of sea ice. J Geophys Res 80:4501–4513

Uttal T et al (2002) Surface heat budget of the Arctic ocean. Bull Am Met Soc 83:255–275

Vavrus S (2004) The impact of cloud feedbacks on Arctic climate under greenhouse forcing. J Clim 17:603–615

Vavrus S (2006) An alternative method to calculate cloud radiative forcing: Implications for quantifying cloud feedbacks. Geophys Res Lett 33:L01805. doi:10.1029/2005GL024723

Vavrus S, Waliser D (2008) An improved parameterization for simulating Arctic cloud amount in the CCSM3 climate model. J Clim 21:5673–5687

Vavrus S, Waliser D, Schweiger A, Francis J (2009a) Simulations of 20th and 21st century Arctic clouds in the global climate models assessed in the IPCC AR4. Clim Dyn 33:1099–1115

Vavrus S, Holland M, Bailey D (2009b) The role of Arctic clouds during intervals of rapid sea ice loss. Community Climate System Model Polar Working Group meeting. Sante Fe, NM

Walsh JE, Portis DH, Chapman WL (2008) Use of ARM/NSA products to evaluate IPCC-AR4 Arctic cloud and radiative simulations. 18th Atmospheric Radiation Measurement (ARM) Science Team Meeting, Norfolk, VA

Wang X, Key JR (2005) Arctic surface, cloud, and radiation properties based on the AVHRR Polar Pathfinder dataset, part II: recent trends. J Clim 18:2575–2593

Wang M, Overland JE (2009) A sea ice-free summer Arctic within 30 years? Geophys Res Lett 36:L07502. doi:10.1029/2009GL037820

Winton M (2006) Does the Arctic sea ice have a tipping point? Geophys Res Lett 33:L23504. doi:10.1029/2006GL028017

Zhang GJ, McFarlane NA (1995) Sensitivity of climate simulations to the parameterization of cumulus convection in the Canadian Climate Centre general circulation model. Atmos Ocean 33:407–446

Zhang M, Lin W, Bretherton CS, Hack JJ, Rasch PJ (2003) A modified formulation of fractional stratiform condensation rate in the NCAR Community Atmospheric Model (CAM2). J Geophys Res 108(D1):4035. doi:10.1029/2002JD002523